Isolated Se_6 Rings in the Voids of a Weakly Interacting, Electroneutral, and Crystalline SiO_2 Matrix: Combined Experimental and Theoretical Study

Gernot Wirnsberger and Harald P. Fritzer

Institute of Physical and Theoretical Chemistry, Technical University of Graz, 8010 Graz, Austria

Robert Zink

Institute of Inorganic Chemistry, Technical University of Graz, 8010 Graz, Austria

Alois Popitsch

Institute of Inorganic Chemistry, Karl-Franzens-University Graz, 8010 Graz, Austria

Bernd Pillep‡ and Peter Behrens*

Institute of Inorganic Chemistry, Ludwig-Maximilians-University Munich, 80333 Munich, Germany

Received: April 12, 1999

For the first time a selenium species has been successfully trapped in the voids of an electroneutral SiO_2 modification, namely, in the porosil decadodecasil 3R (DDR). Raman spectroscopy in combination with theoretical ab initio calculations at the SCF and MP2 levels of theory have been used to assign the observed spectral bands exclusively to Se_6 rings with D_{3d} symmetry. The $A_{1g}(r)$ and $E_g(r)$ mode frequencies of the matrix-isolated Se_6 rings are considerably higher than those of bulk Se_6, suggesting that intermolecular correlations are lost for the perfectly isolated molecules in the microporous host matrix. By an EXAFS analysis of Se *K*-spectra, Se−Se bond lengths of 2.34 Å and next-nearest Se···Se distances of 3.61 Å are obtained, in very good agreement with the theoretical ab initio studies. EXAFS analysis in addition reveals that the interaction between the SiO_2 framework and the embedded Se_6 rings are weak, resulting in a novel host−guest compound with nearly unperturbed Se_6 guest molecules. The crystalline electroneutral host thus acts similarly to a noble gas matrix at low temperatures.

1. Introduction

Microporous compounds, especially zeolites, have attracted much interest with respect to their use as basic host components for the modular assembly of new host−guest compounds [e.g., refs 1−6]. This is due to their regular three-dimensionally assembled pore systems, which are excellently suited for an ordered arrangement of guest molecules. In this respect, the microporous hosts serve as dielectric matrices whereby their pore sizes geometrically confine the space available for the guest components.

Among the elements and compounds inserted into the voids of zeolites, numerous investigations have focused on the incorporation of selenium and the electronic changes associated with the limited size of the occluded Se species. For example, the thermodynamically stable bulk structure, trigonal selenium, is characterized by strong intermolecular interactions between helical $\{^1_\infty\}$Se chains. Through occlusion in zeolites, however, these interactions are lost and bonding distances and band gaps are significantly modified.[7]

So far, investigations in this direction have focused on the inclusion of selenium species in zeolites and $AlPO_4$-5. Despite serious efforts, the occlusion of selenium molecules within the cages and/or channels of microporous SiO_2 modifications in significant amounts proved to be unsuccessful. During our attempts to restructure inorganic materials on a nanometer scale with the help of microporous SiO_2 modifications,[8−10] however, selenium has been successfully introduced into the voids of so-called decadodecasil 3R (structure code: DDR). The structure of the DDR host consists of pseudohexagonal sheets of pentagondodecahedral [5^{12}] cages (Figure 1a), which are stacked in an ABCABC sequence and interconnected by further O−Si−O bridges.[11] By this stacking, larger [$4^3 5^{12} 6^1 8^3$] cages are built up between the sheets (parts b and c of Figure 1). After hydrothermal synthesis, these cages are occupied by 1-aminoadamantane molecules, which act as a structure-directing agent and become occluded during crystallization. By calcination, this molecule can be burned out, leaving the (thermodynamically metastable) SiO_2 matrix with now empty cages behind.

Here, we report our results of the composite material derived by the insertion of selenium into the DDR host structure. This novel host−guest compound has been investigated experimentally by vibrational spectroscopy and EXAFS analysis of Se K-edge spectra. Moreover, computational studies have been performed to support the assignment of the vibrations observed.

2. Experimental Section

2.1. Sample Preparation. The host compound DDR has been prepared and calcined as described in detail previously.[8] For the insertion of selenium, around 0.3 g of the DDR host were

* Corresponding author. Present address: Institute of Inorganic Chemistry, University of Hannover, 30167 Hannover, Germany. E-mail: Peter.Behrens@mbox.acb.uni-hannover.de. Phone: ++49 511 762 3660. Fax: ++49 511 762 3006.

‡ Present address: Patent und Rechtsanwaltskanzlei Kador & Partner, 80469 Munich, Germany.

10.1021/jp991197o CCC: $18.00
Published on Web 06/25/1999

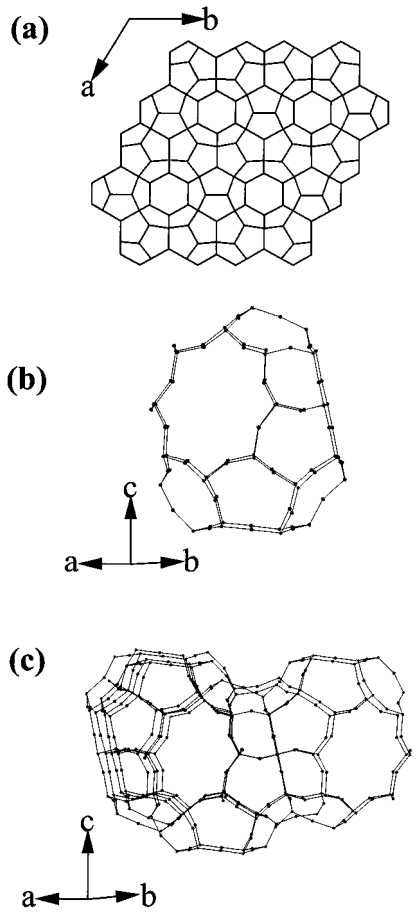

Figure 1. The structure of the silica modification DDR consists of layers of pentagondodecahedra shown in (a). By stacking these layers along the *c* axis and connecting them by Si−O−Si bridges, the characteristic $[4^3 5^{12} 6^1 8^3]$ cages (b) are built up. Each $[4^3 5^{12} 6^1 8^3]$ cage is surrounded by three others at an angle of 120° (c). Note that in (a) oxygens are omitted for clarity.

filled into an 8 mm diameter quartz tube (length 25 cm) and quartz wool was used to fix the host compound. Thereafter, a small capillary containing 1.0 g selenium was put into the quartz tube. After evacuation (10^{-5} bar) at 400 K for 4 h in order to remove remaining water, the quartz tube was closed and heated to 823 K for periods of 6−12 days. During heating, the quartz tube was placed in an oven such that the lower end of the tube held the guest and the DDR host was held by the quartz wool at the upper end. After the reaction time, the tube was cooled to room temperature and opened and the selenium−DDR composite was removed. All samples were stored and measured under ambient conditions.

2.2. Composition and Spectroscopic Measurements. Thermogravimetric analysis (TGA) was employed for the determination of the composition. TGA (run on a Mettler TA 2 thermobalance dynamically under an argon flux of 5 L h^{-1}) reveals mass losses corresponding to unit cell compositions of $120SiO_2 \cdot 8.5Se$ to $120SiO_2 \cdot 12.0Se$ (depending mainly on the crystal size of the used host material).

Raman spectra were obtained at room temperature using equipment consisting of a SPEX 1301 double monochromator, an RCA C31034 photomultiplier tube, photon counting electronics, and a Spectra-Physics model stabilite Ar ion laser operating at 488 nm. Slit widths were chosen to give a resolution of 4 cm^{-1} (at 200 cm^{-1}). To avoid heating effects, the rotating cell technique was applied. Fourier transform (FT) Raman spectra with a resolution of 2 cm^{-1} were collected on a Nicolet FT-Raman 910 spectrometer working in the 180° backscattering geometry; the 1064 nm line of a Nd:YAG laser was used for excitation. Typically, 500 scans were collected with a laser power of ca. 700 mW.

X-ray absorption spectra were recorded at beamline X 1.1 at HASYLAB/DESY in Hamburg (F.R.G.). The storage ring DORIS III was operating at 4.432 GeV with an injection current of 80 mA. The spectrometer is equipped with a Si(311) double-crystal monochromator, and a detuning of the second crystal served to suppress contributions of higher harmonics to the monochromatized beam. The spectra were processed with the program WinXAS.[12] For energy calibration, the first inflection point of the L_3-edge of a simultaneously recorded Pb foil was set to a value of 13.035 keV. The background was modeled using Victoreen-type functions and subtracted from the spectra that were then normalized to give edge jumps $\Delta\mu d$ of approximately 1. To extract the EXAFS signals, cubic spline μ_0-fits were applied to the spectra after conversion into *k*-space. From the Fourier transformed spectra, peaks were backtransformed and fitted with phase and amplitude functions calculated with the program FEFF 7.02.[13]

2.3. Theoretical Calculations. Ab initio calculations were performed with the GAMESS software package employing effective core potentials of Stevens et al.[14] and a double-ζ valence basis with a single polarization function on all selenium atoms (CEP-41G*). Both geometry optimizations and the computation of harmonic frequencies were undertaken at the SCF and MP2 level of theory. Frequencies were obtained by numerical differentiation. The Cartesian coordinates of the equilibrium geometry and the Cartesian Hessian matrix were then input into the ASYM40 program[15] to obtain a description of normal modes in terms of a chosen set of symmetry coordinates. The symmetry coordinates used were those given by Vizi and Cyvin.[16]

3. Results and Discussion

For the elucidation of chalcogen species trapped in microporous host voids, Raman spectroscopy has proven to be a powerful tool.[9,17−24] A typical Raman spectrum of a selenium−DDR composite obtained with the 488 nm line of an Ar^+ laser is shown in Figure 2a (regardless of the composition, which varies slightly with synthesis parameters, the spectra remain unchanged). As usually observed for Raman spectra of microporous compounds, especially pure SiO_2 modifications, a broad luminescence covers almost the whole spectral range of interest. However, three bands at 276, 133, and 102 cm^{-1} are clearly detected (Figure 2b). This observation, together with the fact that none of the bands due to Se_2 (around 392 cm^{-1}) or Se_3 (around 312 cm^{-1}) have been detected, supports the idea of a cyclic selenium species within the host voids. Additional weak features in the Raman spectra can be seen in the range between 270 and 150 cm^{-1}. For this reason, Raman spectra were also collected with near-infrared excitation because under these conditions the disturbing luminescence is strongly suppressed for our composites and only bands due to guest species are detected.[8,9] Despite the fact that this technique is limited to a lower frequency region of around 150 cm^{-1}, the spectra reveal additional information. The high-frequency band centered at 276 cm^{-1} possesses a weak shoulder peaking at 263 cm^{-1} (Figure 3), which (due to its weakness and the low signal-to-noise ratio) is not clearly visible in the spectra recorded with visible light excitation. By comparison with the spectra of the unloaded host, no further bands belonging to the guest species are detected, confirming that the weak modulations of the background that

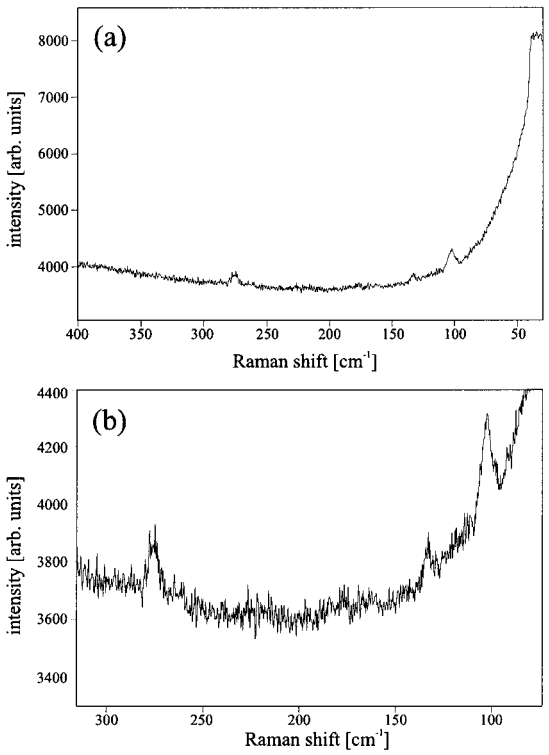

Figure 2. Raman spectrum of selenium inserted in DDR obtained by excitation with the 488 nm line of an Ar ion laser (a). On the broad underlying luminescence, three bands attributable to the selenium guest species are clearly visible (b).

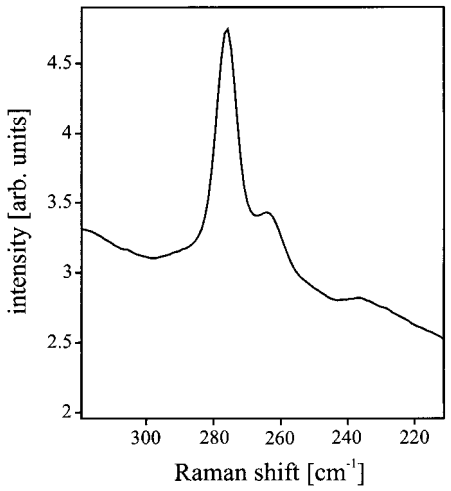

Figure 3. FT Raman spectrum of Se_6 in DDR obtained by excitation with the 1064 nm line of a Nd:YAG laser showing the weak $E_g(r)$ mode at 263 cm^{-1}, which is not visible in Figure 2.

appear in the spectra given in Figure 2 are to be attributed to the SiO_2 framework.

The question to address is which selenium rings are embedded in the $[4^35^{12}6^18^3]$ cages of the host structure. Owing to the geometric confinement imposed by the host, rings consisting of more than six atoms, e.g., the known Se_7,[25] can be excluded and only smaller rings have to be considered. On the other hand, results from our previous investigations on sulfur insertion compounds into the same host structure show that the available space of the voids (free volume of around 350 $Å^3$) is fully occupied by the guest molecules and that larger rings are favored over smaller ones.[9,10] With respect to literature data, it is worth mentioning that bands peaking at around 274, 135, and 104 cm^{-1} have been observed for selenium species inserted into mordenite

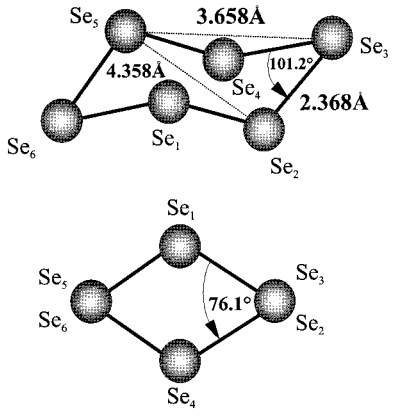

Figure 4. Structural parameters of Se_6 (D_{3d}) as predicted by CEP41G*/MP2 calculations.

TABLE 1: Optimized Geometric Parameters for Se_6 (D_{3d} Symmetry) in Comparison with the Solid-State Structure

	CEP-41G*/SCF	CEP-41G*/MP2	solid Se_6[29]
r_{Se-Se} [Å]	2.345	2.368	2.356 ± 0.009
α [deg]	101.5	101.2	101.1 ± 2.3
ϕ [deg]	75.6	76.1	76.2 ± 2.3

(274, 135, and 104 cm^{-1}),[20,22] $AlPO_4$-5 (104 and 274 cm^{-1}),[23] and zeolite Y[26] (274, 137, and 108 cm^{-1}). These were assigned to Se_6 rings. Very recently, a theoretical calculation of the vibrational spectra of gaseous selenium species supported this assignment.[27] These experimental and computational studies hint to the presence of Se_6 rings in the cages of DDR, too.

For a quantitative assignment of all bands, we performed ab initio calculations for Se_6 rings with D_{3d} symmetry including electron correlation at the CEP-41G*/MP2 level. Our investigations showed that the frequencies obtained at the CEP-41G*/SCF level are close (maximum deviations of 1.8 cm^{-1}) to those predicted at the 6-311G*/SCF level. We therefore assume that treatment of electron correlation at the CEP-41G*/MP2 level yields results similar to results of the 6-311G*/MP2 method (frozen core approximation) and appropriately accounts for some electron correlation in Se_6 (we were unable to compute the frequencies at the 6-311G*/MP2 (frozen core) level because of the limited disk space). The optimized geometric parameters (Table 1) at the SCF and MP2 levels of theory, i.e., bond distances and angles (see also Figure 4), are similar to the values obtained from the single-crystal structure of solid Se_6.[28] In comparison with previous reported theoretical studies, the Se−Se bond distance (2.345 Å on the CEP-41G*/SCF level) is slightly larger than that calculated using the Hartree−Fock method with the 6-31G* basis set[27] (r_{Se-Se} = 2.322 Å) and is close to those predicted by molecular dynamics[29] (r_{Se-Se} = 2.34 Å) and molecular dynamics within the density functional formalism[30] (r_{Se-Se} = 2.35 Å). By use of the optimized geometries, the expected vibrational frequencies for a Se_6 ring with D_{3d} symmetry were calculated. The calculated wavenumbers are listed together with the experimentally observed values and the calculated potential energy distributions (PED) in Table 2 (since Hartree−Fock frequencies are known to be too high by a factor of approximately 0.90, a single scaling factor of 0.92 was chosen for best agreement between calculated and experimental data). As can be clearly seen from Table 1, the inclusion of electron correlation at the MP2 level leads to a significant increase of the Se−Se bond, which causes the calculated Se−Se stretching force constant to decrease from 2.16 (CEP-41G*/SCF) to 1.76 N cm^{-1} (CEP-41G*/MP2). The scaled Hartree−Fock frequencies are in reasonable agreement with

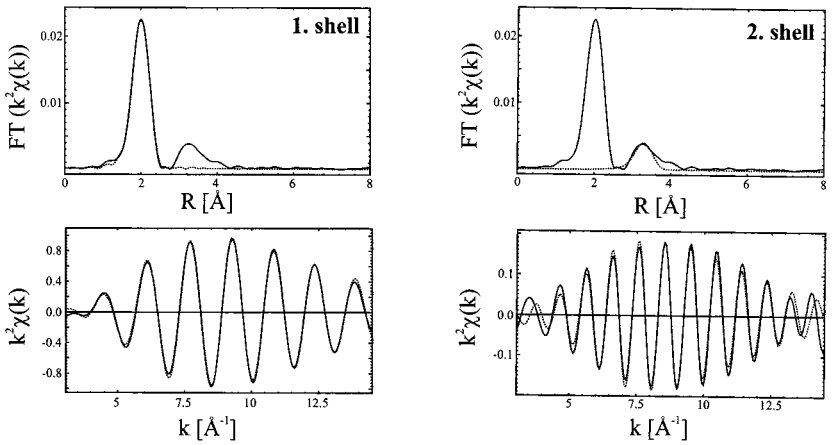

Figure 5. Fourier transforms (top) of the Se K-edge EXAFS spectrum of Se_6 in DDR at 77 K and backtransforms of the two main peaks (bottom). The solid lines depict the experimental curves, and the dotted lines represent the fits for the shell under investigation. Note that the *R* values of the Fourier transforms are not corrected for phase shifts.

TABLE 2: Calculated Frequencies and Potential Energy Distribution (PED) for Se_6 (D_{3d}) and Observed Frequencies for Selenium in DDR (Frequencies Are Given in cm^{-1})

species	vibration	description	CEP-41G*/SCF unscaled	CEP-41G*/SCF scaled by 0.92	CEP-41G*/MP2	observed (Raman)	PED (CEP-41G*/MP2)
A_{1g} (Raman)	ν_1	$A_{1g}(r)$	294.4	271	276.3	276	96(1), 12(2)
	ν_2	$A_{1g}(\alpha)$	139.7	129	130.1	133	90(2), 5(1)
A_{1u} (inactive)	ν_3	$A_{1u}(r)$	294.4	271	239.1		100(3)
A_{2u} (IR)	ν_4	$A_{2u}(\alpha)$	172.5	159	152.3		100(4)
E_g (Raman)	ν_5	$E_g(r)$	302.4	278	266.5	263	107(5), 4(6)
	ν_6	$E_g(\alpha)$	113.9	105	100.1	102	104(6)
E_u (IR)	ν_7	$E_u(r)$	293.2	270	269.0		105(7), 12(8)
	ν_8	$E_u(\alpha)$	86.7	80	80.6		94(8), 1(7)

TABLE 3: Structural Parameters of Se_6 Embedded in DDR Extracted by EXAFS Analysis of Se K-Edge Spectra[a]

shell	r_{Se-Se} [Å]	coordination number	σ^2 [Å^2]	ΔE_0 [eV]	S_0^2	region of backtransformation [Å]	*T* [K]
1	2.34	2*	0.0028	−1.08	1.01	1.43−2.51	77
2	3.610	1.73	0.0057	0.66	1*	2.78−3.64	77
1	2.33	2*	0.0041	−2.08	1.01	1.38−2.50	293
2	3.58	1.45	0.0124	−2.58	1*	2.83−3.50	293

[a] Parameters marked with an asterisk were fixed during fitting. Se−Se distances of the first shell are accurate to ±0.02 Å; for the accuracy of the second-shell data, see text. σ denotes the Debye−Waller factor, ΔE_0 the energy shift, and S_0^2 the amplitude reduction factor.

unscaled frequencies at the MP2 level. However, the A_{1u} mode is clearly overestimated at the SCF level. As can be seen from the PED values, all normal vibrations are well represented by the chosen symmetry coordinates; i.e., the vibrational coupling between symmetry coordinates of the same species is very weak.

By comparison of the frequencies calculated at the MP2 level with those experimentally observed by Raman spectroscopy, the agreement is excellent and confirms the existence of Se_6 rings within the voids of the crystalline matrix.[31] From the close correspondence of the calculated and observed frequencies, it can further be concluded that the occluded Se_6 rings are only weakly perturbed by the force fields of the surrounding SiO_2 framework. The data presented here are also of relevance with respect to the intermolecular bonding in bulk Se_6. In the latter case, the A_{1g} mode has been shown to decrease strongly with increasing pressure,[32] which was interpreted in terms of increasing intermolecular interactions between the individual Se_6 units with increasing pressure. Here, perfectly isolated Se_6 rings can be used to probe the opposite picture; the corresponding A_{1g} and E_g modes are remarkably shifted to higher energies (276 and 263 cm^{-1} against 246 and 221 cm^{-1} for bulk Se_6).[32,33] This result indicates that intermolecular correlations arising from Se···Se contacts of neighboring rings below 4 Å significantly modify the intramolecular bonding in solid Se_6, resulting in a red shift of the corresponding vibrational frequencies in comparison with gaseous or perfectly isolated molecules.

For an investigation of the local structure around the Se atoms, an EXAFS analysis of the Se K-edge X-ray absorption spectra was performed. Figure 5 shows the Fourier transformed EXAFS signal ($\chi(k)\,k^2$) where two main peaks at 2.0 and 3.2 Å can be detected. These peaks were backtransformed into *k*-space and fitted with calculated phase and amplitude functions from FEFF 7.02 (fits are shown in Figure 5).[13] The conditions and results of the fits are given in Table 3.

The values for the nearest Se−Se distances (first shell) with an accuracy of ±0.02 Å are in good agreement with the values calculated for Se_6 rings. The high value of 1.01 for the amplitude reduction factor S_0^2 for both measurements at 77 and 293 K may be attributed to the fact that amplitude-reducing processes and shake-up/shake-off processes[34] are reduced for the occluded Se species as compared to trigonal bulk Se, where the fit (not given in detail) revealed $S_0^2 = 0.8$. The values for the next-nearest Se distances (second shell) obtained by EXAFS are significantly smaller than the calculated values. This is due to the fact that the fits were performed assuming a Gaussian distribution of the Se−Se distances, whereas in reality these are most probably distributed nonharmonically, as already indicated by the nonsymmetric peak shape. In such cases, the

distances obtained with the Gaussian model are too small,[35] and thus, the true value for the next-nearest Se−Se distance is higher than that obtained by the EXAFS analysis. The low coordination numbers found for the second shell reveal the isolated nature of the Se_6 rings located in the cages of the DDR structure. For comparison, from anomalous X-ray scattering experiments on selenium species incorporated in Nd^{3+} exchanged zeolite Y,[36] larger coordination numbers were found for the second shell (4 ± 1) and assigned to weak interactions between these species. Note also that there is no evidence of a contribution of backscattering from O atoms to the EXAFS spectra, as was also observed in the cases of iodine and mercury halide insertion compounds of porosils.[8−10] This is due to the broad distribution of Se−O distances and hence to a high degree of disorder of the guest molecules with respect to the host framework. This can be taken as evidence for very weak host−guest interactions, which in turn supports the view of only minor influences of the SiO_2 host on the occluded Se_6 rings. In summary, the results obtained by the EXAFS analysis further support the presence of perfectly isolated Se rings occluded in the SiO_2 host DDR and also corroborate the calculated structures.

To our knowledge, the composite investigated here is the first example of an insertion compound of selenium in a microporous pure SiO_2 modification. TGA shows the SiO_2 matrix to exhibit a stabilizing effect for the Se_6 rings because mass loss occurs only at relatively high temperatures of around 625 K. For geometric reasons, only small molecules such as Se_2 or Se_3 can leave the matrix (larger molecules are too bulky to pass the eight-membered ring windows of the DDR host structure; see Figure 1). Therefore, this temperature region is assigned to the onset of bond breaking of the Se_6 rings embedded in the DDR host voids. From this point of view, a cautious mechanistic proposal for the elusive isolation of Se_6 rings in DDR may be formulated. At the insertion temperatures of around 823 K, the vapor phase is dominated by Se_2 and Se_3 molecules. These are small enough to penetrate into the 350 $Å^3$ cages. Upon cooling, these small molecules react to cyclic molecules, with the reaction toward Se_6 rings being favored over the formation of smaller ones. However, the geometrical confinement superimposed by the host framework prevents the formation of larger molecules such as Se_7 and Se_8. By the formation of Se_6 molecules, the free space available is used to full extent. Most noteworthy, by use of DDR with only cagelike voids as a host matrix, the formation of selenium chains as they occur in bulk trigonal Se within the host voids is prevented. This shows clearly the templating role of the solid-state matrix toward the elusive isolation and stabilization of Se_6 ring molecules.

4. Conclusions

The chemical vapor deposition of selenium into voids of the crystalline SiO_2 matrix decadodecasil 3R leads to a new host−guest compound with perfectly isolated Se_6 rings within the 350 $Å^3$ cages of the host structure. Both the close correspondence between the vibrational frequencies calculated for gaseous Se_6 rings with D_{3d} symmetry and the experimentally observed ones and structural results from EXAFS analysis confirm that the interactions between the guest species and the SiO_2 framework are very weak. Moreover, the high-temperature stability of the composite material offers the opportunity to study matrix-isolated molecules in a broad temperature range, viz. between the lowest temperatures available up to the selenium desorption starting at 625 K.

Acknowledgment. It is a pleasure to thank HASYLAB for allocating beam time and for the service offered. Moreover, we acknowledge supporting part of this work by the Deutsche Forschungsgemeinschaft and the Fonds der Chemischen Industrie. B.P. is grateful to the Freistaat Bayern for a Ph.D. scholarship.

References and Notes

(1) Stucky, G. D.; MacDougall, J. E. *Science* **1990**, *247*, 669.

(2) Ozin, G. A.; Özkar, S. *Adv. Mater.* **1992**, *4*, 11.

(3) Ozin, G. A. *Adv. Mater.* **1992**, *4*, 612.

(4) Ozin, G. A. *Adv. Mater.* **1994**, *6*, 71.

(5) Herron, N. *J. Inclusion Phenom. Mol. Recognit. Chem.* **1995**, *21*, 283.

(6) Behrens, P.; Stucky, G. D. In *Comprehensive Supramolecular Chemistry*; Alberti, G., Bein, T., Eds.; Pergamon: Oxford, 1996; Vol. 7, p 721.

(7) Parise, J. B.; MacDougall, J. E.; Herron, N.; Farlee, R.; Sleight, A. W.; Wang, Y.; Bein, T.; Moller, K.; Moroney, L. E. *Inorg. Chem.* **1988**, *27*, 221.

(8) Wirnsberger, G.; Fritzer, H. P.; Popitsch, A.; van de Goor, G.; Behrens, P. *Angew. Chem.* **1996**, *108*, 2951; *Angew. Chem., Int. Ed. Engl.* **1996**, *35*, 2777.

(9) Wirnsberger, G.; Fritzer, H. P.; van de Goor, G.; Pillep, B.; Behrens, P.; Popitsch, A. *J. Mol. Struct.* **1997**, *410−411*, 123.

(10) Wirnsberger, G. Ph.D. Thesis, Technical University of Graz, Graz, Austria, 1998.

(11) Gies, H. *Z. Kristallogr.* **1986**, *175*, 93.

(12) Ressler, T. *J. Phys. IV* **1997**, *7*, 269.

(13) Zabinsky, S. I.; Rehr, J. J.; Ankudinov, A.; Albers, R. C.; Eller, M. J. *Phys. Rev. B* **1995**, *52*, 2995.

(14) Stevens, W. J.; Krauss, M.; Basch, H.; Jasien, P. G. *Can. J. Chem.* **1992**, *70*, 612.

(15) Hedberg, L.; Mills, I. M. *J. Mol. Spectrosc.* **1993**, *160*, 117.

(16) Vizi, B.; Cyvin, S. J. *Acta Chem. Scand.* **1968**, *22*, 2012.

(17) Poborchii, V. V. *J. Phys. Chem. Solids* **1994**, *55*, 737.

(18) Lindner, G.-G.; Hoffmann, K.; Witke, K.; Reinen, D.; Heinemann, C.; Koch, W. *J. Solid State Chem.* **1996**, *126*, 50.

(19) Poborchii, V. V.; Ivanova, M. S.; Petranovskii, V. P.; Barnakov, Y. A.; Kasuya, A.; Nishina, Y. *Mater. Sci. Eng. A* **1996**, *217/218*, 129.

(20) Poborchii, V. V. *Chem. Phys. Lett.* **1996**, *251*, 230.

(21) Goldbach, A.; Saboungi, M.-L.; *Ber. Bunsen-Ges. Phys. Chem.* **1997**, *101*, 1660.

(22) Poborchii, V. V.; Kolobov, A. V.; Oyanagi, H.; Romanov, S. G.; Tanaka, K. *Chem. Phys. Lett.* **1997**, *280*, 10.

(23) Poborchii, V. V.; Kolobov, A. V.; Caro, J.; Zhuravlev, V. V.; Tanaka, K. *Chem. Phys. Lett.* **1997**, *280*, 17.

(24) Goldbach, A.; Iton, L. E.; Saboungi, M.-L. *Chem. Phys. Lett.* **1997**, *281*, 69.

(25) Takahashi, T.; Yagi, S.; Sagawa, T.; Nagata, K.; Miyamoto, Y. *J. Phys. Soc. Jpn.* **1985**, *54*, 1018.

(26) Goldbach, A.; Grimsditch, M.; Iton, L.; Saboungi, M.-L. *J. Phys. Chem. B* **1997**, *101*, 330.

(27) Kohara, S.; Goldbach, A.; Koura, N.; Saboungi, M.-L.; Curtis, L. A. *Chem. Phys. Lett.* **1998**, *287*, 282.

(28) Miyamoto, Y. *Jpn. J. Appl. Phys.* **1980**, *19*, 1813.

(29) Oligschleger, C.; Jones, R. O.; Reimann, S. M.; Schober, H. R. *Phys. Rev. B* **1996**, *53*, 6165.

(30) Hohl, D.; Jones, R. O.; Car, R.; Parrinello, M. *Chem. Phys. Lett.* **1987**, *139*, 540.

(31) For a complete comparison, an experimental elucidation of the three IR frequencies would be desirable. However, no bands corresponding to the guest species have been detected by far-IR measurements on comparison with the unloaded host, owing to the dominating broad absorptions of the SiO_2 framework and the (relatively) low concentration of the guest species.

(32) Nagata, K.; Ishikawa, T.; Miyamoto, Y. *Jpn. J. Appl. Phys.* **1983**, *22*, 1129.

(33) Nagata, K.; Ishibashi, K.; Miyamoto, Y. *Jpn. J. Appl. Phys.* **1981**, *20*, 463.

(34) Teo, B. K. *EXAFS: Basic Principles and Data Analysis*; Springer: Berlin, 1986.

(35) Crozier, E. D.; Rehr J. J.; Ingalls, R. In *X-ray Absorption*; Koningsberger, D. C., Prins, R., Eds.; Chemical Analysis 92; Wiley: New York, 1988; Chapter 9.

(36) Armand, P.; Saboungi, M.-L.; Price, D. L.; Iton, L.; Cramer, C.; Grimsditch, M. *Phys. Rev. Lett.* **1997**, *79*, 2061.